


DELIVERABLE 4.4.1	
CONTRACT N°	SPC8-GA-2009-233655
PROJECT N°	FP7-233655
ACRONYM	CITYHUSH
TITLE	Acoustically Green Road Vehicles and City Areas
Work Package 4	Propagation attenuation of road traffic noise
4.4	Reduction of low frequency structure borne noise
	Propagation barrier - concept
Written by	Hamid Masoumi D2S
Due submission date	31-12-2011
Actual submission date	15-01-2012
Project Co-Ordinator Partners	Acoustic Control ACL SE Accon ACC DE Alfa Products & Technologies APT BE Goodyear GOOD LU Head Acoustics HAC DE Royal Institute of Technology KTH SE NCC Roads NCC SE Stockholm Environmental & Health Administration SEP SE Netherlands Organisation for Applied Scientific Research TNO NL Trafikkontoret Göteborg TRAF SE TT&E Consultants TTE GR University of Cambridge UCAM UK Promotion of Operational Links with Integrated Services POLIS BE
Project start date	January 1, 2010
Duration of the project	36 months Project funded by the European Commission within the Seventh Framework program Dissemination Level PU Public ✓ PP Restricted to other programme participants (including the Commission Services) RE Restricted to a group specified by the consortium (including the Commission Services) CO Confidential, only for the members of the consortium (including the Commission Services)
	Nature of Deliverable
	R Report ✓
	P Prototype
	D Demonstrator
	O Other

TABLE OF CONTENTS

1	Executive summary	3
1.1	Objective of the deliverable.....	3
1.2	Description of the work performed since the beginning of the project	3
1.3	Main results achieved so far	3
1.4	Expected final results.....	3
1.5	Potential impact and use.....	4
1.6	Partners involved and their contribution.....	4
1.7	Conclusions	4
2	Traffic-induced vibration Mitigation.....	5
3	Mitigation at low frequency	6
4	One-dimensional modeling of the Vibration reduction mechanism.....	8
5	Numerical prediction of the barrier efficiency	12
6	Test bench configuration.....	15
7	Measurement setup.....	22
8	References	23

1 EXECUTIVE SUMMARY

1.1 OBJECTIVE OF THE DELIVERABLE

Design solutions to reduce low frequency vibrations and structure-borne noise from heavy vehicles (busses and trucks passing over bumps and uneven pavement).

1.2 DESCRIPTION OF THE WORK PERFORMED SINCE THE BEGINNING OF THE PROJECT

1. Investigation on a reliable, efficient and applicable isolating system for the traffic-induced vibrations
 - A literature study was done to find an appropriate mitigation system.
 - An analytical study of possible solutions was done to find the important parameters, which influence the efficiency of the isolating system.
 - A numerical tool has been prepared for modelling of the isolating system. The numerical model can account for the road-soil interaction, the wave transmission through the ground, and the structure of the isolating barrier.
2. Constructing a physical model of the isolating system as a reduced-scale test bench to confirm the efficiency of the designed system and to validate the results of the proposed numerical method:
 - Selecting an appropriate scale factor and proper dimensioning of the system and the scaled frequency range.
 - Soil investigation after the sand deposition in the test bench container.
 - Selecting a relevant measurement configuration: the vibration source, type of accelerometers and their positions.
 - The barrier fabrication.

1.3 MAIN RESULTS ACHIEVED SO FAR

The literature study as well as the numerical modelling of the problem reveal that among several types of barriers, a multi-layer barrier with a stiff-soft-stiff configuration would be very efficient at low frequencies.

1.4 EXPECTED FINAL RESULTS

1.5 POTENTIAL IMPACT AND USE¹

1.6 PARTNERS INVOLVED AND THEIR CONTRIBUTION

1.7 CONCLUSIONS

A multi-layer isolating barrier has been examined numerically and then, a three-layer barrier consisting of two concrete walls and a middle EPS layer is designed. Results of the numerical modelling show that a three-layer barrier would be more efficient than a one-layer barrier with the same characteristics. In both vertical and the horizontal response, a reduction factor of around 0.2 to 0.3 is obtained for excitation frequencies higher than 10 Hz.

¹ including the socio-economic impact and the wider societal implications of the project so far

2 TRAFFIC-INDUCED VIBRATION MITIGATION

The traffic-induced vibrations, in an urban area may, damage the building, give annoyance to the people and cause malfunctioning to sensitive equipment in nearby buildings. The study of ground-borne vibrations and their effects on the nearby structures has received considerable attention and concern during the last two decades, [1, 2, 3].

The problem of traffic-induced vibration mitigation by barriers is termed as a dynamic soil-structure interaction problem together with a wave scattering and wave transmission mechanism.

The characteristics of the propagating waves induced by an excitation on the ground surface show the existence of three types of the elastic waves (figure 1). Body waves (shear and compression waves) are most dominant in the soil and propagate in all directions on a spherical wave front. Rayleigh waves however propagate radially on a cylindrical wave front along the surface.

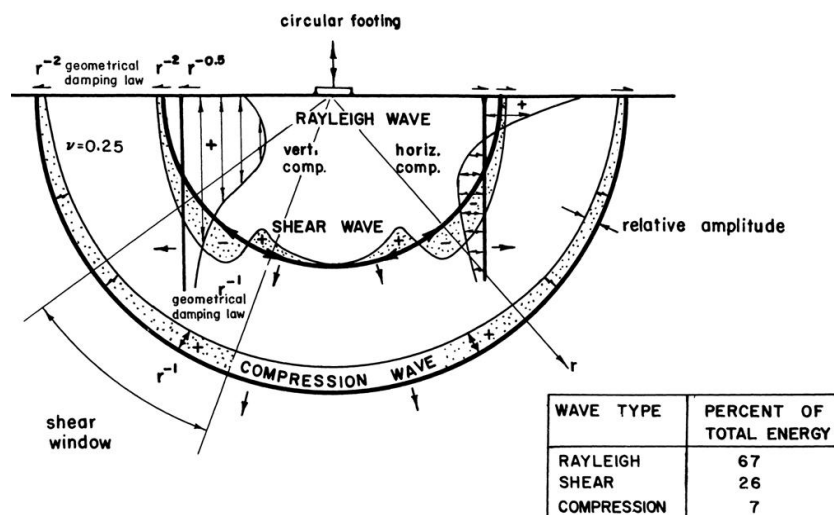


Figure 1

Distribution of stress waves from a circular footing on a homogeneous half space (after Woods [4])

Most of the vibration energy affecting nearby buildings and structures is carried by Rayleigh waves propagating in a zone close to the ground surface. According to Woods [4], for a vertical excitation of a circular footing, around 67% of the input energy is transmitted by Rayleigh waves.

This energy can be reduced by installing a wave barrier system against the wave propagating direction. This results in reflection, damping and scattering of the incoming waves.

The isolating systems can be classified by their position such that a system installed close to the source is called an active isolation and that installed inside or near to the building (receiver) is a passive isolation. In the present work, an active isolation is considered.

Traffic-induced vibrations are mainly due to the interaction between the vehicle (wheels) and the road surface. The dynamic axle loads are determined by the vehicle dynamics, the road unevenness and the road flexibility [5, 6, 7]. According to

Pyl et al. (2004) [5], the axle's peak acceleration increases almost linearly with increasing vehicle speeds. However, this trend is not observed for the rear axle. Further, the dominant frequency of generated ground vibrations is mainly determined by the axle hop modes of the vehicle as well as the type of the road unevenness and is not influenced by the vehicle speed.

Figure 2 shows the time history and the frequency content of the ground velocity measured at 16 m from the road on the surface due to the passage of a truck at a speed $v = 50$ km/h on an artificial plywood unevenness and the joint between two concrete plates. In both cases, the response presents the frequency content below 60 Hz. Furthermore, results display that the unevenness of the road influences the dominant frequency of the ground motions such that a dominant frequency of 12 Hz and 18 Hz is observed respectively for the plywood unevenness and for the joint on a concrete road.

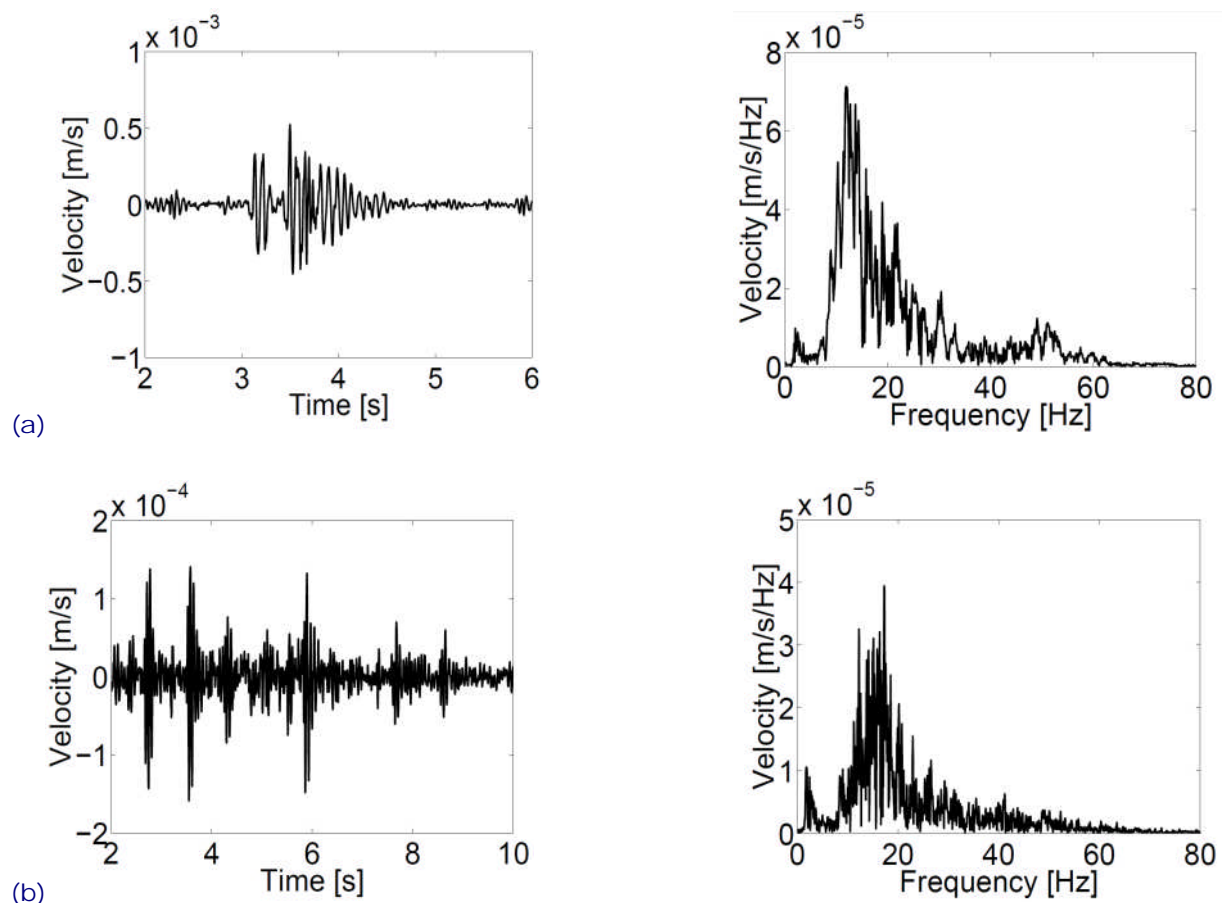


Figure 2

Time history and frequency content of the velocity measured at 16 m from the road on the ground surface generated by the passage of a truck at a speed $v = 50$ km/h
(a) on an artificial plywood unevenness and
(b) on the joint between two concrete plates (after Pyl et al. [5])

An investigation on the experimental measurements shows that the passage of heavy trucks generates vibrations at a frequency range from 10 to 30 Hz, [3, 5, 8]. Therefore, the main focus in this work would be on the mitigation of vibrations in this frequency range.

3 MITIGATION AT LOW FREQUENCY

The problem of traffic-induced vibration mitigation by barriers is termed as a dynamic soil-structure interaction problem, together with a wave scattering and wave transmission mechanism.

The problem is decomposed into three sub-problems:

1. the excitation mechanism and the vehicle-load-soil interaction,
2. the wave transmission through the soil and the soil-barrier interaction,
3. the soil-building interaction.

The generated dynamic impact force of tires on the pavement surface is mainly related to the type of pavement (the pavement roughness and irregularities), the tire bounce (the vehicle dynamic system), and the vehicle speed. Since the road is much stiffer than the vehicle's suspension or tyres, the dynamic axle loads are independent of the soil characteristics. Hence, to predict the free field vibrations due to traffic-induced vibrations, the vehicle-road-soil interaction problem may be decoupled into a vehicle-road and a road-soil interaction problem, Lombaert et al. [6].

The ground motions encountered by the building foundation propagate into the building's elements such as the walls and the floors. The vertical vibration of the floors could be significantly higher than that received at the foundation level, [5, 6].

The characteristics of the propagating waves due to road traffic show the existence of two types of elastic waves: body waves (shear and compression waves) and surface waves (Rayleigh and Love waves). Body waves are mostly dominant in the soil and propagate in all directions on a spherical wave front. Rayleigh waves (surface waves) however propagate radially on a cylindrical wave front along the surface. The vibration amplitude in the free field naturally reduces with distance from the source because of the geometrical and material damping.

A vibration mitigation system may act in three ways: (1) reducing the vibration amplitude by improving the soil around the vibration source, (2) increasing the frequency content of the induced vibrations and (3) reducing the energy of the transmitted wave.

The emphasis of this work is on the second and the third way and considers an isolating barrier. The presence of an isolating barrier between the vibration source and the receivers can reduce the vibration level at the receiver points by reflecting and scattering the incoming waves as well as by reducing the wavelength of the incoming waves by wave modulation of the barrier layers.

The isolating barriers can also be classified by the location of the barrier; the isolating system, near to the source, is referred to as "active isolation" and that in the proximity of the structure is referred to as "passive isolation". Since the waves at lower frequencies (longer wavelength) attenuate slowly with distance, an active isolating system would be more effective as a countermeasure of induced vibrations at low frequency.

In designing an efficient isolating barrier, the main objective would be to shift the frequency of the induced waves into higher ones (smaller wavelength) as well as reducing the vibration amplitude by the impedance jump between the layers.

4 ONE-DIMENSIONAL MODELING OF THE VIBRATION REDUCTION MECHANISM

An isolating barrier can consist of only one or multiple layers of different materials, [8, 9]. Takemiya (2004) [8], has proposed a wave impeding soil-columns barrier as a honeycomb WIB. In the frequency range below the cut-off frequency of the system, no wave transmission occurs through the soil in the outer zone (far field), while in the frequency range above it, the resonance of the layers may amplify ground motions. Based on soil properties and the excitation frequencies expected from high-speed trains, the proposed honeycomb WIB, significantly reduces the vibration level in a shallow zone close to the source.

To better understanding and figuring out the mechanism of vibration reduction by multi-layer barriers, the isolating system is modelled by one-dimensional wave propagation.

Figure 3 shows the scheme of a one layer and a multi-layer barrier. A set of parallel layers with different material properties is considered. Each layer has a thickness " d ", shear wave velocity " C " and density " ρ ".

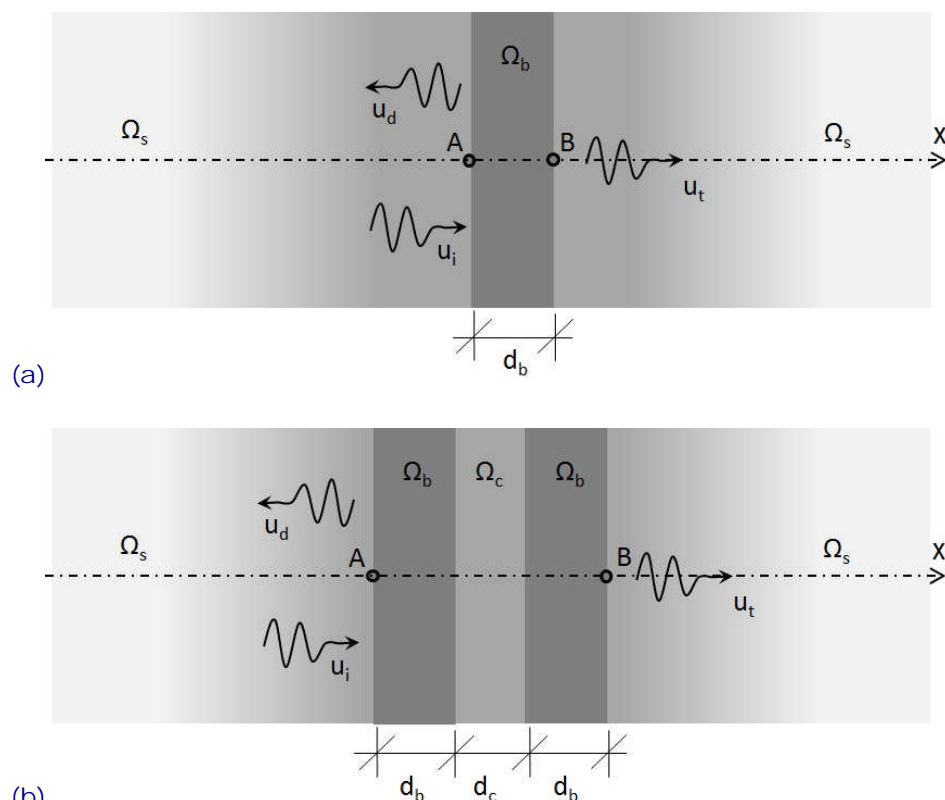


Figure 3

Scheme of one-dimensional modelling of (a) a one-layer barrier and (b) a three-layer barrier

The efficiency of the isolating system is defined by the reduction factor “ A_r ” as the ratio between the transmitted wave amplitude to that of the incident wave:

$$A_r = u_t / u_i$$

With a one-dimensional wave propagation model, it can be shown that the reduction factor “ A_r ” depends on:

1. the impedance ratio $\alpha = \rho_b C_b / \rho_s C_s$ as: $A_r \propto \frac{1}{(\alpha + \frac{1}{\alpha})}$
2. and, the travelling time $t_b = d_b / C_b$ as: $A_r \propto \frac{1}{t_b}$

In summary, for a more efficient barrier, an impedance ratio far from unity (much higher than 1 or very smaller than 1) and a longer time travelling are needed. In the following, the influence of the impedance ratio as well as the travelling time is investigated on the efficiency of an isolating barrier.

Using EDT toolbox in MATLAB [10], a numerical simulation has been performed to compute the transmitted “ u_t ” as well as the diffracted wave field “ u_d ” due to a unit harmonic incident wave “ u_i ” at point A, see figure 4. The direct stiffness method proposed by Kausel [11], is employed to solve the equation of motion of the system.

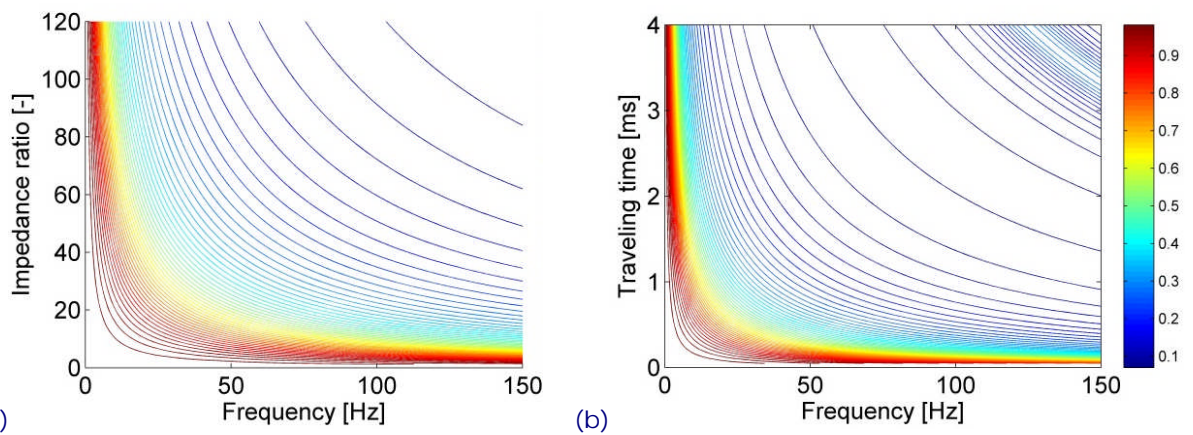


Figure 4

(a) Reduction factor versus excitation frequency for
 (a) variant impedance ratio and constant travelling time, and for
 (b) constant impedance ratio and variant travelling time

In addition, it can be shown that a combination of multi-layer barrier would be more efficient than a one layer barrier. A multi-layer barrier originates a cut-off frequency phenomenon based on the resonance frequencies of the barrier layers.

In a multi-layer barrier, a combination of multiple impedance jump mechanisms and the cut-off frequency phenomenon due to the wave modulation of the middle layers results in an effective amplitude reduction.

According to Takemiya (2004) [8], repeating of the layers in the barrier decreases the wave transmissibility in an exponential decay as: $A_r^n \cong (A_r)^N$, where N denotes to the number of layer repetition and A_r is the reduction factor obtained by one layer barrier.

Figure 5 shows the amplitude reduction factor calculated for four cases: the one-layer barrier (soil-concrete-soil) and three three-layer barriers.

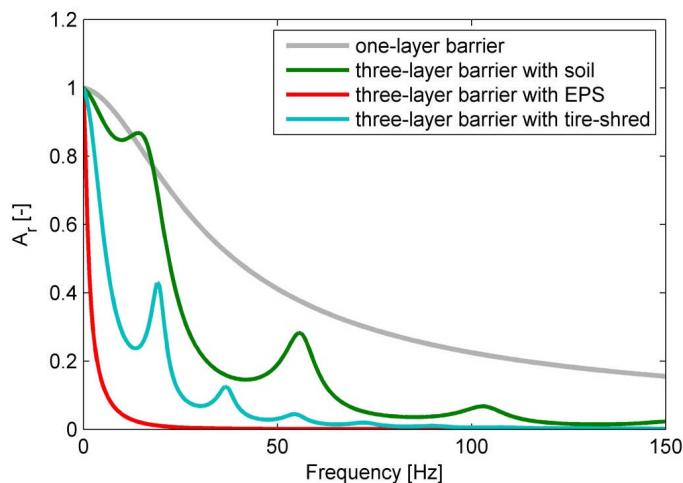


Figure 5

Reduction factor computed for a one-layer of concrete barrier (thick grey line) and that of three-layer barriers with soil, extruded polystyrene, and tire-shred (thin lines)

Results are obtained for different middle layers of soil, extruded polystyrene (EPS), and tire-shred with impedance ratios $Z_{concrete}/Z_{soil} = 30$, $Z_{concrete}/Z_{EPS} = 3200$, and $Z_{concrete}/Z_{tire-shred} = 105$, where Z denotes to the mechanical impedance such that : $Z_a = \rho_a C_a$, table 1.

Material	Young modulus [MPa]	Poisson's ratio [-]	Density [kg/m ³]	Damping ratio [%]
Concrete	30 000	0.25	2500	1
Soil	100	0.33	1800	5
EPS [8]	2	0.15	12	5
Tire-shred [12]	5	0.40	1400	5

Table 1 The properties of the materials used

In all cases, the middle layer has a thickness $d = 1.0$ m. Figure 5 displays how a combination of layers in the isolating barrier results in increased efficiency. The best efficiency is observed for the case with extruded polystyrene.

For a three-layer barrier in a stiff-soft-stiff configuration, a significant reduction is observed above the resonance frequency of the first mode. This frequency changes with the material properties used in the soft middle layer. For the three-layer barrier

with soil (concrete-soil-concrete), the first mode at 20 Hz and higher modes at around 55, 105 Hz are observed. For the second and the third modes, the frequencies at 53 and 103 Hz correspond to the vibration modes of the middle layer (the soil): $f_n \approx n C_b / 2d_b$ for $n \geq 2$.

Furthermore, results show that among different barriers, the concrete-EPS-concrete would be the most efficient one. Celebi et al. (2009) [9] came to similar conclusions. Employing a concrete-box barrier filled by different soft materials, they performed a set of experimental measurements in full scale. They showed that a softer backfill material results in a higher efficiency of the isolating barrier.

It should be noted that the one-dimensional modelling cannot take into account for the influence of the barrier depth and at least a two-dimensional modelling is required to study the effects of the barrier depth.

5 NUMERICAL PREDICTION OF THE BARRIER EFFICIENCY

In practice, the construction of a very deep barrier becomes more difficult and consequently, more expensive with increasing depth. A parametric study is done using a numerical model. The objective of this study is to show how a three-layer barrier with a middle soft layer would be more efficient than a deeper one-layer barrier. Figure 6 illustrates the lay-out of the two barrier types.

A two-dimensional coupled FE-BE modelling with 2D plane strain elements is considered. The plane strain elements are selected to reduce the cost and the time of the computation. In addition, the 2D Green's functions of a layered half space have been employed for the boundary element computation. The green's functions are evaluated by means of the direct stiffness method, [10, 11].

A coupled finite element-boundary element method has been used, in which the barrier and the track are modelled by FEM and the soil impedance as well as the free field vibrations is computed by BEM.

The barrier is a concrete wall that has a height H_b , a thickness W_b and is located at distance R_b from the vibration source: a slab track, figure 6a.

The three-layer barrier consists of two concrete walls. The space between the walls is filled by the extruded-polystyrene (EPS), figure 6b.

The concrete has a Young's modulus $E_c = 30,000$ Mpa, a Poisson's ratio $\nu_s = 0.25$, and a material density $\rho_c = 2,500$ kg/m³.

The extruded-polystyrene has a Young's modulus $E_e = 2$ Mpa, a Poisson's ratio $\nu_e = 0.15$, and a material density $\rho_e = 12$ kg/m³, [8].

The soil medium is a homogeneous half space with Young's modulus $E_s = 200$ Mpa, a Poisson's ratio $\nu_s = 0.33$, a material density $\rho_s = 1,800$ kg/m³, and a material damping $\beta_s = 5\%$. The shear and compression wave velocities of the soil are 200 m/s and 400 m/s, respectively. According to the material properties, the impedance ratio concrete to soil and concrete to EPS are 15 and 3200, respectively.

A frequency analysis has been done by applying a unit vertical force on the concrete slab. The slab is assumed rigid and mass-less.

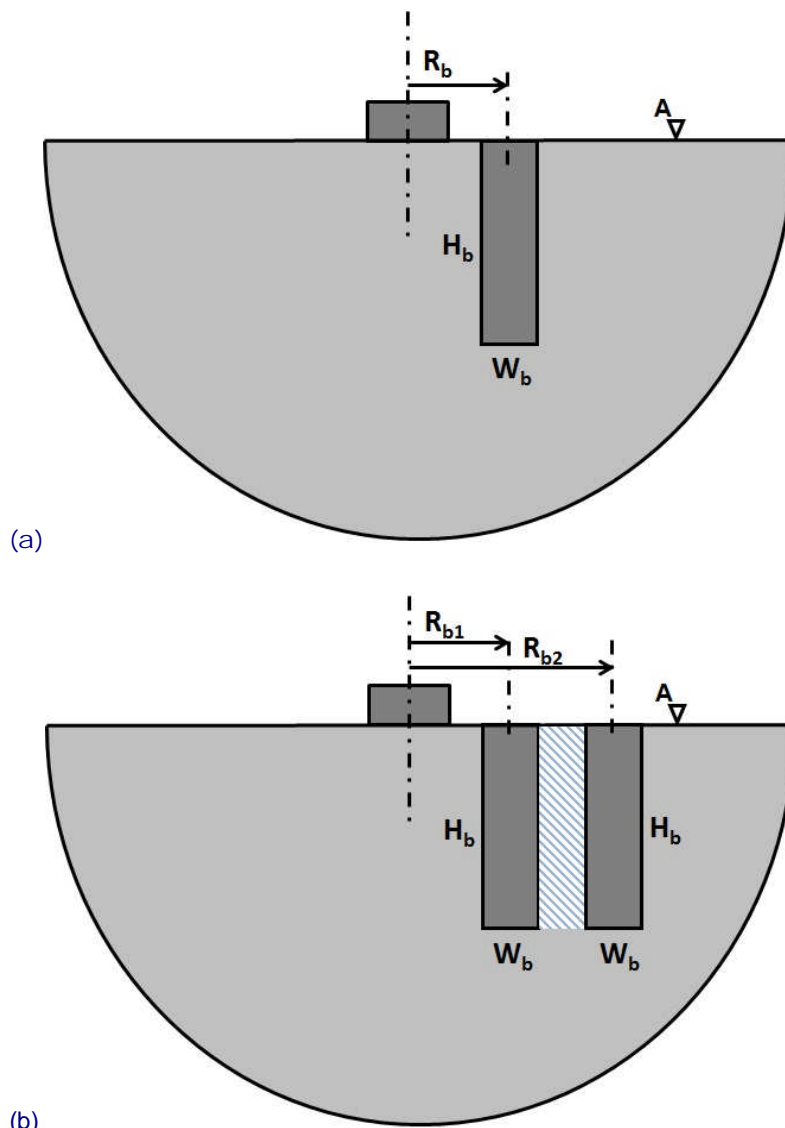


Figure 6

Overview of the isolating system: (a) one-layer barrier and (b) three-layer barrier with a middle layer

Free field vibrations are compared for different cases. The soil responses are calculated for the reference case where no barrier exists. Then, a one-layer barrier with depth $H_b = 20$ m and two three-layer barriers with $H_b = 5$ and 10 m are modelled. The barriers have width $W_b = 0.5$ m and are located at the same distance from the source.

Figure 7 shows the variation of the peak particle velocity (PPV) on the soil surface versus the distance from the source at 20 and 50 Hz. The results computed for the different barrier configurations are compared with the reference case (without barrier). At 20 Hz, higher attenuation is observed when a three-layer barrier with depth $H_b = 10$ m is employed. At 50 Hz, very high attenuation is obtained by all barriers.

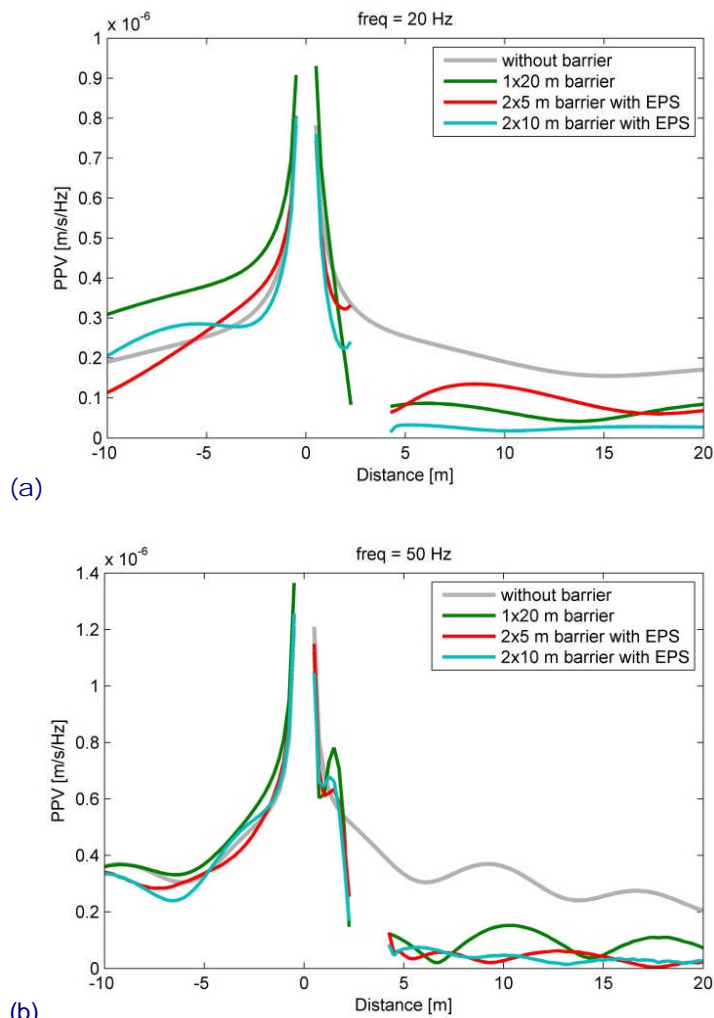


Figure 7

(b) Peak particle velocity (PPV) on the soil surface versus distance from the source at (a) 20 and (b) 50 Hz, computed for different barrier configuration

Figure 8 shows the mobility function on the soil surface at 10 m from the source. The results again show that the three-layer barrier with depth $H_b=10$ m decreases very well the vibration amplitude for frequencies higher than 10 Hz.

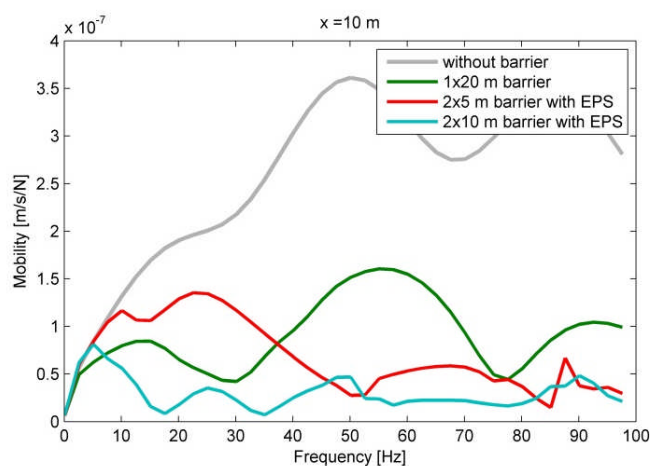


Figure 8

Mobility function on the soil surface at 10 m from the source, computed for different barrier configuration

Woods [1] has proposed a criterion to evaluate the efficiency of trenches (barriers) by introducing the Amplitude Reduction Factor. The amplitude reduction factor A_r for a certain point is defined as the ratio between the vibration amplitude after the installation of the trench (isolated response) to that measured before the installation of the trench (unisolated response):

$$A_r = u_{isolated} / u_{unisolated} \quad (1)$$

The amplitude reduction factors are calculated for different cases. Results shown in figure 9 clearly confirm the results of the one-dimensional modelling presented in the previous section that a three-layer barrier would be more efficient than a one-layer barrier with the same characteristics. In both vertical and the horizontal response, a reduction factor of around 0.2 to 0.3 is obtained for excitation frequencies higher than 10 Hz. According to Woods [1], an efficient isolating system must result in a reduction factor below than 0.25, which is equivalent to an insertion loss of 12 dB.

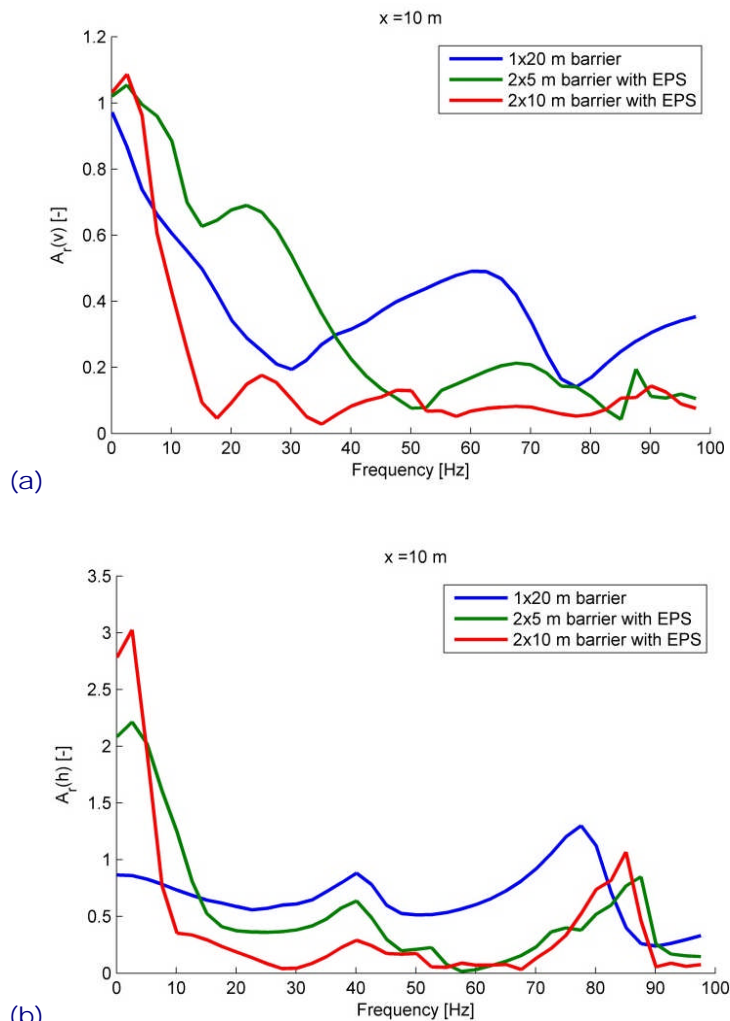


Figure 9

(a) Vertical and (b) horizontal reduction factor versus excitation frequency in a point located at 10 m from the source, computed for different barrier configuration

6 TEST BENCH

To improve the results of the numerical prediction model, a physical modelling of the isolating problem has been designed as a small-scale test. The test bench consists of (1) a soil container, (3) an isolating screen (a barrier), and (3) soil (a clean fine sand).

Some difficulties for realizing the boundary conditions in the test bench are resolved by selecting an appropriate scaling factor as well as a relevant dimension for the soil container. On the other hand, considering the soil container's size and the dominant frequency of the induced vibrations, a scaling factor must be chosen, [13].

Since traffic induced vibrations are dominant in a frequency range from 10 to 30 Hz, the isolating system must be effective around this frequency range. Therefore, a set of numerical computations were performed to find a reasonable scaling factor and consequently an effective isolating barrier dimension in the frequency range of interest.

Physical unit	Model/Prototype
Length w, d, r	$1/N$
Frequency	N
Time	$1/N$
Velocity	1
Acceleration	N
Wavelength	$1/N$
Dimensionless length $w/\lambda, d/\lambda, r/\lambda$	1
Acoustic impedance Z	1
Density	1
Force	$1/N^2$

Table 2 Scale factors used in the physical modelling

The selected soil is the Mol silica sand, type M32 from SIBELCO, with an average grain size (D50) of 0.26 mm and a dry density of 1700 kg/m³. The sand is very well sieved, washed and then dried and classified.

Investigating on different soil preparation methods shows that the pluviation method or sand raining is an efficient tool for providing a uniform and homogeneous sand specimen. The pluviation method is less operator-dependent and more repeatable than the other methods such as the moist tamping, dry tapping and pouring using a hand-rotated flask. Furthermore, results of the pluviation method show more uniformity in density and void ratio in the sand when compared to the other methods, [14, 15, 16].

The container is a box with a floor, and four sidewalls with dimensions 2 m x 4 m x 2 m that has been filled with the sand with a 1.5 m depth. The walls are made by deformed galvanized-steel plates with 0.75 mm thickness. Interior of the container, sidewalls and the floor have been covered by wooden plates to achieve a proper smooth surface.



Figure 10

Overview of the sand pluviation in the container

The filling with sand has been done using the pluviation device that moves on two rails over the container with a speed of approximately 0.18 to 0.2 m/s. The height of the sand drop is varied from 10 to 25 cm.

The pluviation device consists of three main parts: a tank or reservoir in the upper level to deliver the sand through a nozzle, a shutter that can be in open/close position to control the delivery of sand. The shutter consists of a fixed perforated plate and a sliding plate. Opening the sliding plate lets the sand pass through the holes in the perforated plate, and a diffuser with a guide box and two grids (sieves). The second grid is positioned at the lower part of device and its holes have different directions to polarize the drop.

The density of pluviated sand depends on fall height, depositional intensity, and uniformity of the sand rain. The influence of fall height on sample density has been investigated by several researchers, [14, 15].

The soil density was investigated. During pluviation, 16 receptacles were installed at depths of 40 cm, 20 cm and on the surface of the sand. The receptacles have been distributed along the container width at distances of 40 cm and 60 cm from the container wall. Results show average densities of 1640 at the surface, 1685 at 20 cm depth and 1700 kg/m³ at 40 cm depth, figure 11. The results of these tests will be used in the numerical modelling.

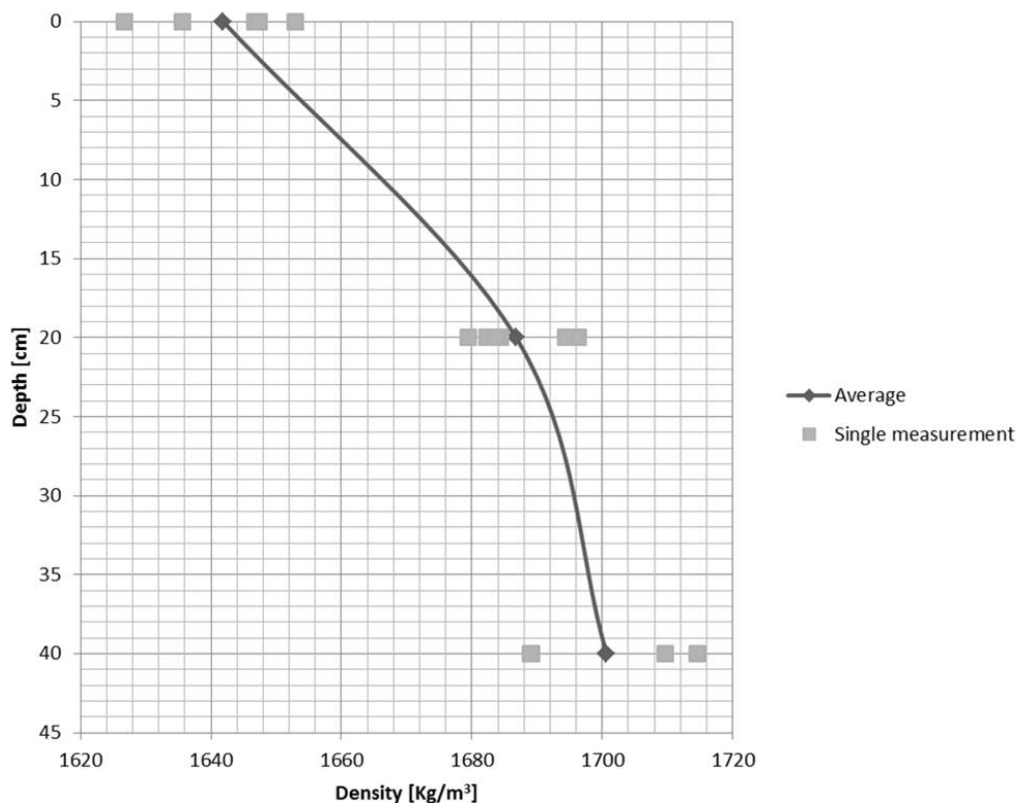


Figure 11

Variation of sand density prepared by pluviation versus the depth in the container

In addition, upon completion of the soil pluviation, the uniformity of the soil stiffness (at the top layer) is examined by the impedance test. The test configuration consists of a small steel foundation, two accelerometers installed on the foundation, and a hammer, figure 12.

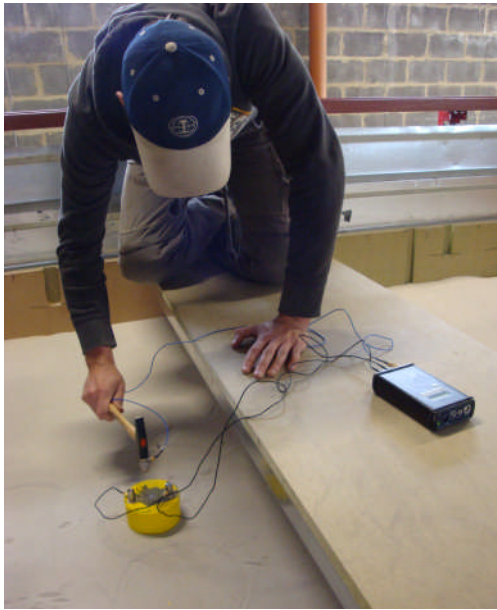


Figure 12

Impedance test setup using a hammer impact on the foundation

Then, the response to the hammer impact is measured by a small rigid foundation posed on the soil surface. A set of points on the sand surface has been selected for the test. Figure 12 shows an overview of the test; figure 13 of the position of the measurement points.

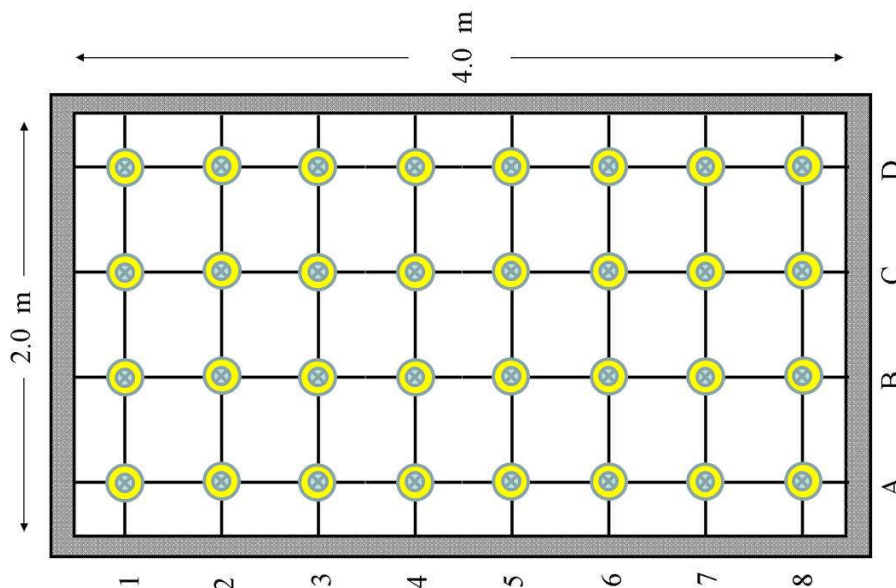


Figure 13

Overview of the impedance test and the position of the measurement points in the container

Since the foundation is rigid, the dynamic foundation-soil system can be defined with a model of one degree of freedom with the foundation mass and the soil impedance. So, the resonance frequency of the system is determined as:

$$f_n = \frac{1}{2\pi} \sqrt{\frac{K_v}{M_f}} \quad (2)$$

Where K_v denotes to the vertical soil impedance and, M_f is the mass of the foundation.

The resonance frequency of the system can be obtained directly from the foundation response where the response reaches its maximum. Therefore, for the given foundation mass and the frequency resonance of the system, the soil impedance can be calculated by the equation (2). The vertical soil impedance of a circular rigid foundation can be analytically defined as:

$$K_v(a_0) = \frac{4Gr}{1-\nu} [k(a_0) + ic(a_0)] \quad (3)$$

where $k(a_0)$ and $c(a_0)$ are the dynamic coefficients, $a_0 = \omega r / C_s$ is the dimensionless frequency and, G, ν , and r are the soil shear modulus, soil Poisson's ratio and the foundation radius, respectively.

For dimensionless frequency $a_0 < 0.25$, the vertical soil impedance is frequency independent, [17], such that:

$$K_v \cong \frac{4Gr}{1-\nu} \quad (4)$$

Therefore, replacing the equation (4) into the equation (2), the shear modulus of the soil is obtained.

Figure 14 shows the mobility function of the foundation due to the impact hammer. Results presented for all measurement points, show a resonance frequency range from 110 to 115 Hz.

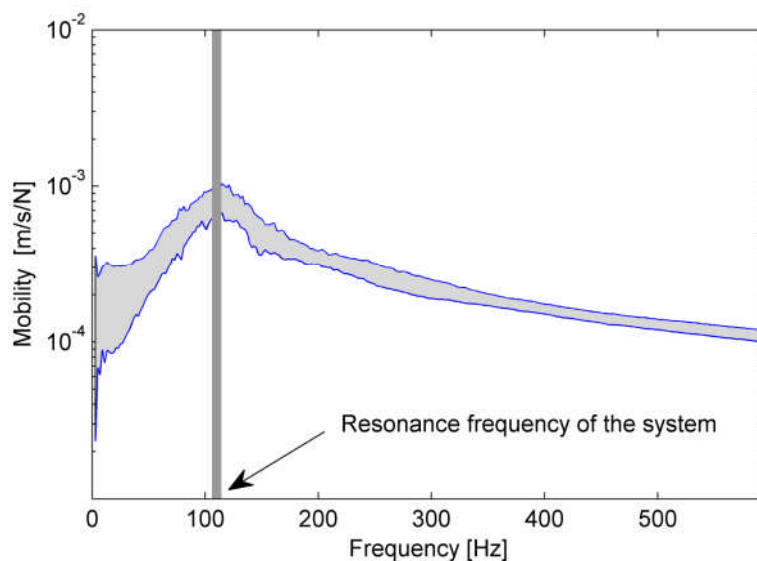


Figure 14

Mobility functions of the foundation

Figure 15 displays the distributions of the shear modulus over the soil surface. Results are calculated by means of equations (2) and (4) for $r = 5$ cm, $\nu = 0.3$ and the foundation mass $M_f = 3150$ g. The results show that the shear modulus around the centreline of the container is uniformly distributed with an average value of 7.5 MPa. Near the sidewalls, however, soil rigidity is not uniformly distributed.

The sand properties (the density and the shear modulus) measured by the density test and the impedance test will be used in the numerical modelling.

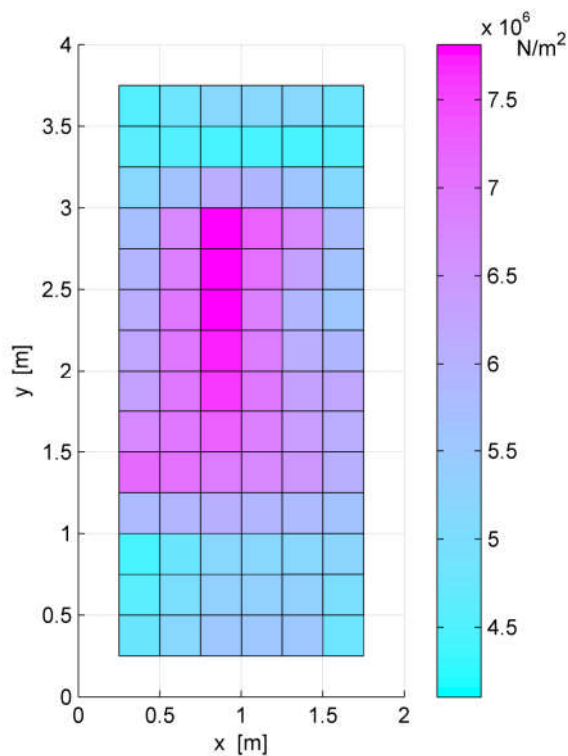


Figure 15

Distributions of the shear modulus measured by the impedance test

7 MEASUREMENT SETUP

The measurement configuration consists of a small foundation posed on the soil surface where the dynamic force is applied and accelerometers mounted at the measurement points. The barrier is installed at a specific distance on one side from the foundation. The small foundation is excited at the frequency band of interest and the free field vibrations are measured at the different points.

The accelerometers are located on the soil surface symmetrically on both sides of the foundation. This configuration enables us to simultaneously measure with the same soil and excitation condition, the un-isolated response (on the side without the barrier) and the isolated response (on the side where the barrier is installed).

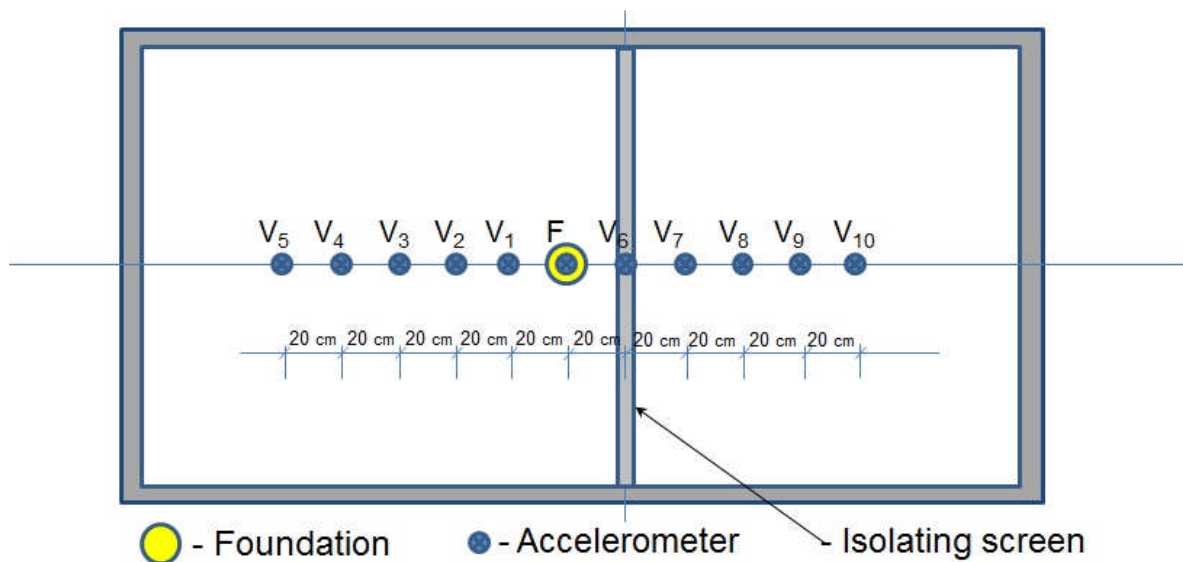


Figure 16

Overview of the measurement setup

A shaker device is used for the excitation generation. The shaker is installed over a small foundation. The type, the amplitude and the frequency content of the excitation can be controlled by means of a wave generator software that feeds into a power amplifier. A random vibration from 100 to 1100 Hz is used.

The free field response at the unisolated side is considered as the reference vibration. To obtain the isolation efficiency of the isolating barrier, the results of this reference vibration are compared with those measured at the isolated side.

A set of experimental measurements in small-scale are planned to validate the predicted results of the numerical modelling.

8 REFERENCES

- [1] S. François, L. Pyl, H. Masoumi, G. Degrande. The influence of dynamic soil-structure interaction on traffic induced vibrations in buildings. *Soil Dynamics and Earthquake Engineering*, 27 (7), 655-674, 2007.
- [2] A. T. Peplow and A. M. Kaynia. Prediction and validation of traffic vibration reduction due to cement column stabilization. *Soil Dynamics and Earthquake Engineering*, 27:793–802, 2007.
- [3] K.R. Massarsch. Mitigation of traffic-induced ground vibration. In *Proceedings of the 11th International Conference on Soil Dynamics and Earthquake Engineering*, Berkeley, California, USA, June 2004.
- [4] R.D. Woods. Screening of surface waves in soils. Technical report, University of Michigan, Industry program of the college of engineering, January 1968.
- [5] L. Pyl, G. Degrande, G. Lombaert, W. Haegeman. Validation of a source-receiver model for road traffic-induced vibrations in buildings. I: Source model. *Journal of engineering mechanics-asce*, 130 (12), 1377-1393, 2004.
- [6] G. Lombaert, G., Degrande. The experimental validation of a numerical model for the prediction of the vibrations in the free field produced by road traffic. *Journal of sound and vibration*, 262 (2), 309-331, 2003.
- [7] M. Lak, G. Degrande, G. Lombaert. The effect of road unevenness on the dynamic vehicle response and ground-borne vibrations due to road traffic. *Soil Dynamics and Earthquake Engineering*, 31 (10), 1357-1377, 2011.
- [8] D.S. Kim and J.S. Lee. Propagation and attenuation characteristics of various ground vibrations. *Soil Dynamics and Earthquake Engineering*, 19:115–126, 2000.
- [9] H. Takemiya. Field vibration mitigation by honeycomb WIB for pile foundations of a high-speed train viaduct. *Soil Dynamics and Earthquake Engineering*, 24:69–87, 2004.
- [10] E. C. elebi, S. Firat, G. Beyhan, I. Cankaya, I. Vural, and K. Osman. Field experiments on wave propagation and vibration isolation by using wave barriers. *Soil Dynamics and Earthquake Engineering*, 29:824–833, 2009.
- [11] M. Schevenels, S. François, and G. Degrande. EDT: An ElastoDynamics Toolbox for MATLAB. *Computers & Geosciences*, 35(8):1752–1754, 2009.
- [12] E. Kausel. *Fundamental solutions in elastodynamics: a compendium*. Cambridge University Press, New York, 2006.
- [13] K. Itoh, X. Zeng, O. Murata, and O. Kusakabe. Centrifugal simulation on vibration reduction generated by high-speed trains using rubber-modified asphalt foundation and EPS barrier. *International Journal of Physical Modelling in geotechnics*, 2:1–10, 2003.
- [14] J. Garnier, C. Gaudin, S.M. Springman, P.J. Culligan, D. Goodings, D. Konig, B. Kutter, R. Phillips, M.F. Randolph, and L. Thorel. Catalogue of scaling laws and similitude questions in geotechnical centrifuge modelling. *International Journal of Physical Modelling in geotechnics*, 7(3):1–24, 2007.
- [15] S. Miura and S. Toki. A sample preparation method and its effect on static and cyclic deformation-strength properties of sand. *sf*, 22(1):61–77, 1982.
- [16] Y. P. Vaid, S. Sivathayalan, and D. Stedman. Influence of specimen-reconstituting method on the undrained response of sand. *gtj*, 22(3):187–195, 1999.
- [17] R. Lagioia, A. Sanzeni, and F. Colleselli. Air, water and vacuum pluviation of sand specimens for the triaxial apparatus. *sf*, 46(1):61–67, 2006.
- [18] J.G. Sieffert and F. Cevaer. *Handbook of impedance functions, surface foundations*, Ouest editions, 1991.